Chinese Chemical Letters 36 (2025) 109795

Contents lists available at ScienceDirect

Chinese Chemical Letters

journal homepage: www.elsevier.com/locate/cclet

Flexible polyphosphazene nanocomposite films: Enhancing stability and luminescence of $CsPbBr_3$ perovskite nanocrystals

Husitu Lin[a], Shuangkun Zhang[a], Dianfa Zhao[a], Yongkang Wang[a], Wei Liu[a], Fan Yang[d,*], Jianjun Liu[c,*], Dongpeng Yan[b,*], Zhanpeng Wu[a,*]

[a] State Key Laboratory of Organic-Inorganic Composites, Beijing University of Chemical Technology, Beijing 100029, China
[b] Beijing Key Laboratory of Energy Conversion and Storage Materials, College of Chemistry, Beijing Normal University, Beijing 100875, China
[c] State Key Laboratory of Chemical Resource Engineering, Beijing University of Chemical Technology, Beijing 100029, China
[d] School of Chemistry & Chemical Engineering and Environmental Engineering, Weifang University, Weifang 261061, China

ARTICLE INFO

Article history:
Received 31 January 2024
Revised 13 March 2024
Accepted 19 March 2024
Available online 19 March 2024

Keywords:
Polyphosphazene
$CsPbBr_3$
Quantum dots
Encapsulation
Luminescent properties
High stability

ABSTRACT

Polyphosphazene with phenoxy or 4-ester phenoxy as pendent groups are demonstrated as both ligands and host matrices for $CsPbBr_3$ perovskite nanocrystals (NCs). These polymers produced flexible nanocomposite films with excellent NCs dispersion, optical transparency and stability in various extreme conditions. Both films remained stable even after 30 days of air storage. $CsPbBr_3$/poly[bis(phenoxy phosphazene)] (PBPP) delivered better air and light stability, and $CsPbBr_3$/poly[bis(4-esterphenoxy) phosphazene] (PBEPP) exhibited superior water and heat resistance. $CsPbBr_3$/PBEPP showed a greater increase in fluorescence intensity under 365 nm UV light and demonstrated a 10% luminescence increase after 96 h of water immersion and even at high temperature (150 °C). These findings thus provide new insight into flexible luminescent $CsPbBr_3$ films with high stability in optoelectronic applications.

The term "quantum dots (QD)" applicable in the semiconductor nanocrystals that features the size on the order of excitonic Bohr radius [1,2]. QDs [3,4] have gained much attention in the fields of solar cells, laser photon detectors, and light-emitting diodes (LEDs), by virtue of their excellent photoluminescence quantum yields (PLQY) and narrow emission bandgap. During the past several years, lead halide perovskite quantum dots (PQDs) with a general formula of ABX_3 (where A = Cs, methylamine; B = Pb, Sn; X = Cl, Br, I) were extensively explored due to their tunable and efficient photoluminescence (PL) properties [5–9]. Unfortunately, these nanocrystals are highly unstable under environmental conditions, such as humidity, UV radiation, oxygen, heat, and polar solvent, which largely restrict their usage in long-term applications on industrial scale [10,11].

A number of strategies have been employed to boost the stability of PQDs, including ion doping [12], surface passivation [13], coating [14], and the addition of organic polymers [15–17]. Surface passivation is considered as a highly effective technique for achieving improved stability. Aggregation can be prevented effectively by introducing hydrophobic organic ligands, and defects on the surface of PQDs can be effectively passivated. In a recent study, Qiu *et al.* used a wide range of aromatic carboxylic acids as ligands for $CsPbBr_3$ PQDs [18]. These PQDs displayed minimal reduction of photoluminescence intensity at ambient conditions and maintained their stability up to 100 h. Another strategy involves polymeric encapsulation of PQDs, by using polymethylmethacrylate (PMMA), polystyrene (PS) and ethylene vinyl acetate (EVA), which can improve their water resistance, mechanical performance and luminescent properties. Furthermore, to achieve stabilization of PQDs, polymer matrices must possess comprehensive properties, such as high transparency, excellent hydrophobicity, high thermal stability, and UV resistance.

In comparison with traditional polymers with carbon backbones, polyphosphazenes are comprised of a versatile family of polymer built on –[P=N]– [19] backbones owing to high reactivity, which can be linked to a wide range of side chains [20,21]. This leads to the product with a similarly diverse range of physical and chemical properties. Polyphosphazenes have excellent thermal stability, high chain flexibility, high refractive index, flame retardant, biocompatible and optical transparency, which make them suitable to be applied in the fields of biomedical engineering, energy generation and storage, and aerospace materials [22–26]. The nitrogen element [27] in backbone and the functional group at the side group exhibit coordination inter-

* Corresponding authors.
E-mail addresses: 18813193360@163.com (F. Yang), liujj@mail.buct.edu.cn (J. Liu), yandp@bnu.edu.cn (D. Yan), wuzp@mail.buct.edu.cn (Z. Wu).

https://doi.org/10.1016/j.cclet.2024.109795
1001-8417/

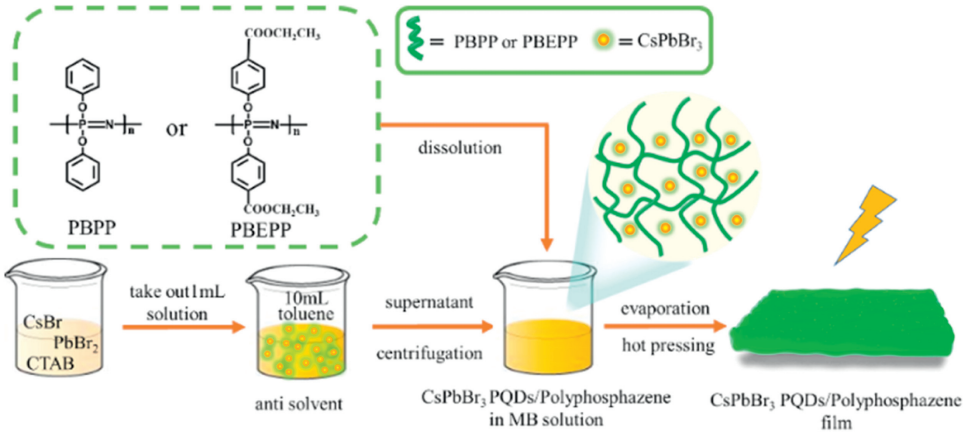

Scheme 1. Schematic illustration of preparation of $CsPbBr_3$/polyphosphazene thin films.

actions with the metal nanoparticle and prevent their agglomeration. Poly(bis(phenoxy)phosphazene) (PBPP) [28] is a type of high-performance organic materials with excellent light stability, thermal stability, hydrophobicity and barrier properties. Simultaneously, poly(bis(4-esterphenoxyl)phosphazene) (PBEPP) [29] not only exhibits high light and chemical stability, but also can enhance the interface bonding strength between the metal ions and polyphosphazenes. Our group previous research has shown that some polyphosphazenes with aromatic side groups own higher fluorescence performance as well, which demonstrate the combination of $CsPbBr_3$ PQDs and polyphosphazenes matrices may lead to a synergetic effect with enhanced luminescence. They both own conjugated structures that favor the charge transport, and the additional electron-withdrawing groups (like ester-phenoxyl) can also tailor the electronic structures and energy levels [30].

In this work, we highlight the use of linear polyphosphazenes as both ligand and encapsulation material for PQDs. By utilizing coordinating groups like main-chain nitrogen and side-chain oxygen, the surface defects of $CsPbBr_3$ can be passivated effectively. The PQDs were uniformly dispersed within the polymer matrix. As a result, $CsPbBr_3$ QDs/PBPP and $CsPbBr_3$ QDs/PBEPP flexible composite thin films were successfully fabricated (Scheme 1). These films demonstrated exceptional resistance abilities to a wide range of environments, such as water, UV light, high temperature and oxygen. Furthermore, the performance of two different phenoxy side group on PQDs was conducted. The high-performance composite thin films with remarkable transparence and flexibility in this study has strong applied potential in the field of luminescence and optoelectronics.

Fig. 1a shows the toluene solutions of $CsPbBr_3$ PQDs/PBPP and $CsPbBr_3$ PQDs/PBEPP under sunlight, showing the uniform dispersion of PQDs in the polymer solution. These solutions remain clear and transparent, and exhibit significant fluorescence intensity under 365 nm UV light irradiation (Fig. 1d). The $CsPbBr_3$ PQDs/PBPP and $CsPbBr_3$ PQDs/PBEPP films, which are prepared through the film casting method, display transparency after the solvent is evaporated at 75 °C. When exposed to ultraviolet light, they emit bright green light (Figs. 1b and e). This result proved that there is no phase separation between $CsPbBr_3$ PQDs and polyphosphazenes, and the structure of $CsPbBr_3$ PQDs is not destroyed, during the heating and film formation processes, which can be further confirmed by the confocal fluorescence microscopy results (Fig. 2). The prepared polymer films also exhibit high flexibility and can be bent for many times (Figs. 1c, e and f), making them suitable for further processing and utilization.

The XRD patterns (Fig. 3) of $CsPbBr_3$ PQDs shows three distinct peaks at approximately 15.1°, 21.5° and 30.5°, which can be

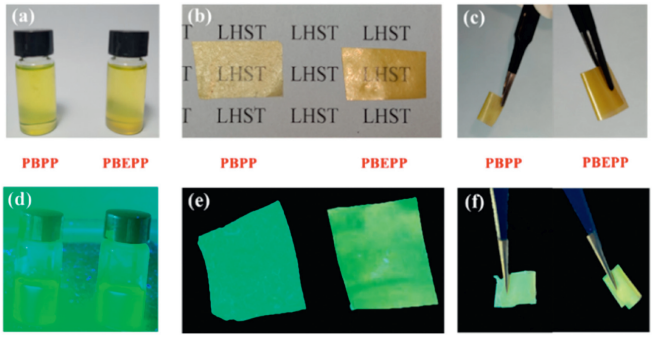

Fig. 1. Photographs of (a, d) $CsPbBr_3$ PQDs/PBPP-toluene and $CsPbBr_3$ PQDs/PBEPP-toluene. (b, e) $CsPbBr_3$ PQDs/PBPP and $CsPbBr_3$ PQDs/PBEPP thin films. (c, f) $CsPbBr_3$ PQDs/PBPP and $CsPbBr_3$ PQDs/PBEPP thin films after bending. (a-c) Under daylight and (d-f) under UV (365 nm) light, respectively.

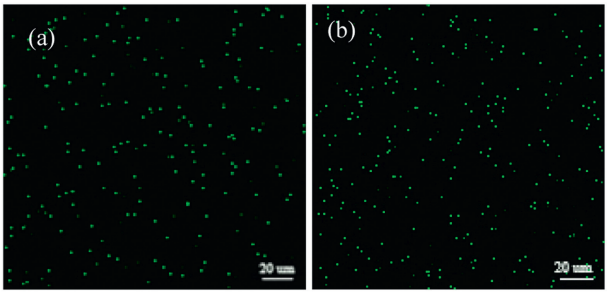

Fig. 2. Fluorescence images of (a) $CsPbBr_3$ PQDs/PBPP and (b) $CsPbBr_3$ PQDs/PBEPP thin film.

attributed to the (100), (110) and (200) crystal planes, respectively. These peaks are consistent with the reference JCPDF No. 18-0364. Additionally, the composite films ($CsPbBr_3$ PQDs/PBPP and $CsPbBr_3$ PQDs/PBEPP) also exhibit characteristic diffraction peaks from $CsPbBr_3$ PQDs. This indicates that the $CsPbBr_3$ PQDs have been successfully encapsulated in the polymer matrix, and their crystal structure remains intact without any damage.

In the FT-IR spectrum of $CsPbBr_3$ PQDs (Fig. 4) [31], the peaks observed at around 2925 cm^{-1} and 2847 cm^{-1} are attributed to the symmetric and antisymmetric C–H stretching vibrations, respectively. For $CsPbBr_3$ PQDs/PBPP and $CsPbBr_3$ PQDs/PBEPP, the spectra show prominent characteristic peaks of $CsPbBr_3$ PQDs, indicating the successful embedding of $CsPbBr_3$ PQDs into PBPP and PBEPP polymers. For the PBPP, the peak at 1200 cm^{-1} is assigned to the –N=P– stretching vibration [32], while for the $CsPbBr_3$

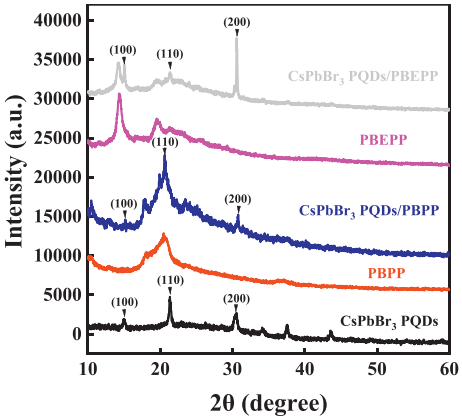

Fig. 3. XRD patterns of the PBPP, PBEPP, pristine $CsPbBr_3$ PQDs, $CsPbBr_3$ PQDs/PBPP and $CsPbBr_3$ PQDs/PBEPP thin films.

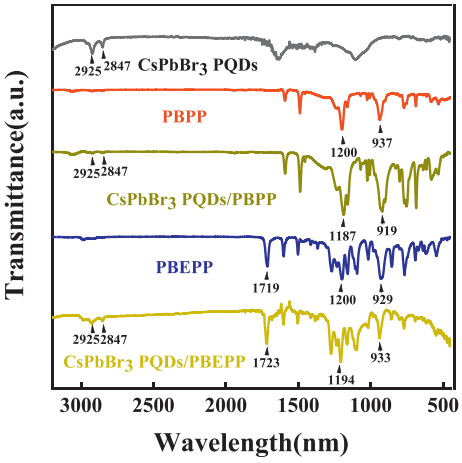

Fig. 4. FT-IR spectra of the PBPP, $CsPbBr_3$ PQDs/PBPP, PBEPP and $CsPbBr_3$ PQDs/PBEPP thin film.

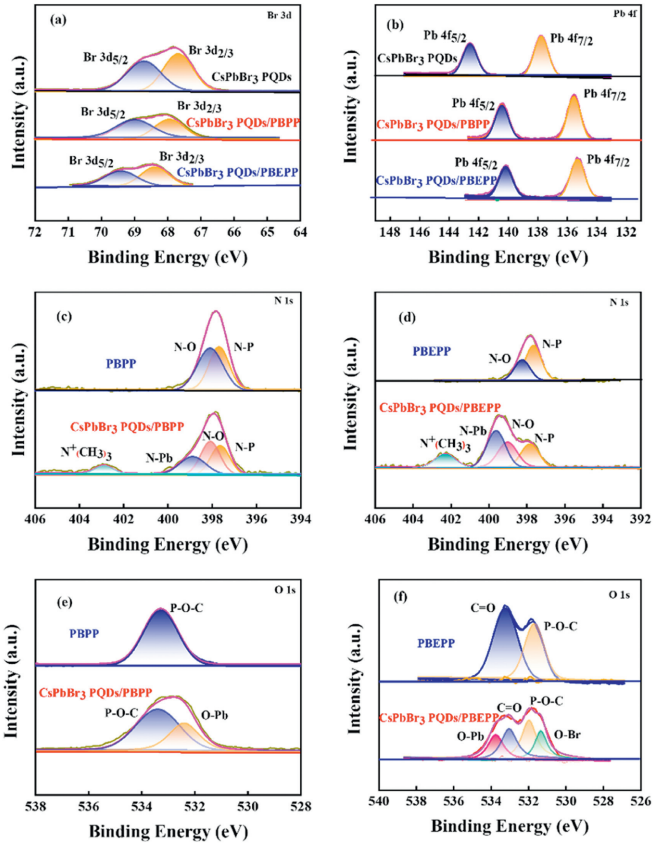

Fig. 5. (a) Br 3d and (b) Pb 4f XPS spectra of $CsPbBr_3$, $CsPbBr_3$ PQDs/PBPP and $CsPbBr_3$ PQDs/PBEPP thin film. (c, d) N 1s and (e, f) O 1s XPS spectra of $CsPbBr_3$ PQDs/PBPP and PBPP thin film, $CsPbBr_3$ PQDs/PBEPP and PBEPP thin film.

PQDs/PBPP, a blue shift of the –N=P– stretching vibration is observed at 1187 cm^{-1}. Similarly, comparing the –N=P– stretching vibration peaks of PBEPP [33] and $CsPbBr_3$ PQDs/PBEPP, a blue shift is also observed from 1200 cm^{-1} towards 1194 cm^{-1}. This is due to the coordination effect between the N/P of the polyphosphazenes backbone and $CsPbBr_3$ PQDs. In the PBPP infrared spectrum, the peak at 937 cm^{-1} is attributed to the stretching vibration of –P–O–, while in the $CsPbBr_3$ PQDs/PBPP spectrum, this feature peak is blue-shifted to 919 cm^{-1}. Similarly, comparing PBEPP and $CsPbBr_3$ PQDs/PBEPP, the –P–O– peak shifts from 929 cm^{-1} to 933 cm^{-1}, indicating the coordination effect between the oxygen in –P–O– and $CsPbBr_3$ PQDs. In the FT-IR spectrum of PBEPP, the peak at 1719 cm^{-1} is assigned to the stretching vibration of –C=O–. In the $CsPbBr_3$ PQDs/PBEPP spectrum, this peak is red-shifted to 1723 cm^{-1}, which is attributed to the coordination betweenbase the –C=O– in the side groups of PBPP and $CsPbBr_3$ PQDs [34]. The strong interactions between polymers (PBPP or PBEPP) and $CsPbBr_3$ PQDs have effectively prevented the aggregation of PQDs in the polymer matrix and enabled their stable.

In order to further investigate the interactive mechanism between $CsPbBr_3$ PQDs with polymers, XPS analysis was performed on $CsPbBr_3$ PQDs/PBPP and $CsPbBr_3$ PQDs/PBEPP [31,34]. As shown in Fig. 5a, the high-resolution XPS spectrum of perovskite Br 3d can be deconvoluted into two peaks at 68.74 and 67.64 eV, which can be assigned to Br $3d_{5/2}$ and Br $3d_{3/2}$, respectively. However, in $CsPbBr_3$ PQDs/PBPP, the corresponding binding energies of Br $3d_{5/2}$ and $3d_{3/2}$ are located at 69.04 eV and 67.94 eV, respectively. In $CsPbBr_3$ PQDs/PBEPP, the binding energies are 69.45 and 68.35 eV, respectively, which have been shifted to higher field. The Pb 4f XPS spectra exhibits two peaks at 142.64 and 137.84 eV corresponding to Pb $4f_{5/2}$ and Pb $4f_{7/2}$, respectively (Fig. 5b). Similarly, in $CsPbBr_3$ PQDs/PBPP and $CsPbBr_3$ PQDs/PBEPP, they have undergone a shift towards lower field at 140.44 eV ($4f_{5/2}$), 135.54 eV ($4f_{7/2}$) and 140.14 eV ($4f_{5/2}$), 135.34 eV ($4f_{7/2}$), respectively. Based on the electron shielding effect, as the electron density increases around an atom, the binding energy decreases accordingly. These results confirm that the interaction between $CsPbBr_3$ PQDs with polymers has profound effect in electron environment around $CsPbBr_3$, which leads to a decrease in the electron density of Pb and an increase in the electron density of Br. In addition, the side group structures of polymer have significant influence on the interaction between $CsPbBr_3$ PQDs with polyphosphazenes. Strong molecular interaction is distinguished $CsPbBr_3$ PQDs with PBEPP from $CsPbBr_3$ PQDs with PBPP.

In the $CsPbBr_3$ PQDs/PBPP, the N 1s spectrum (Fig. 5c) can be divided into four major peaks at 397.65 eV (N=P), 398.15 eV (N–Br), 398.95 eV (N–Pb) and 402.75 eV ($N^+(CH_3)_3$). The O 1s spectrum (Fig. 5e) exhibits three peaks at 533.15 eV (P–O), 533.95 eV (O–Pb) and 532.35 eV (O–Br). As displayed in Fig. 6, the results above indicate that there are hydrogen bond and coordination effect between Br/Pb from the PQDs and N/O in the main chain of the polyphosphazene [35]. This result is consistent with FT-IR spectra. Meanwhile, the N 1s and the O 1s spectra of the composite film shows the same binding energy of N=P and P–O–C with pure polymer, the chemical structure of polyphosphazenes in composite film does not change. Furthermore, similar behaviors are also observed in the O 1s and the N 1s spectra of $CsPbBr_3$ PQDs/PBEPP (Figs. 5d and f).

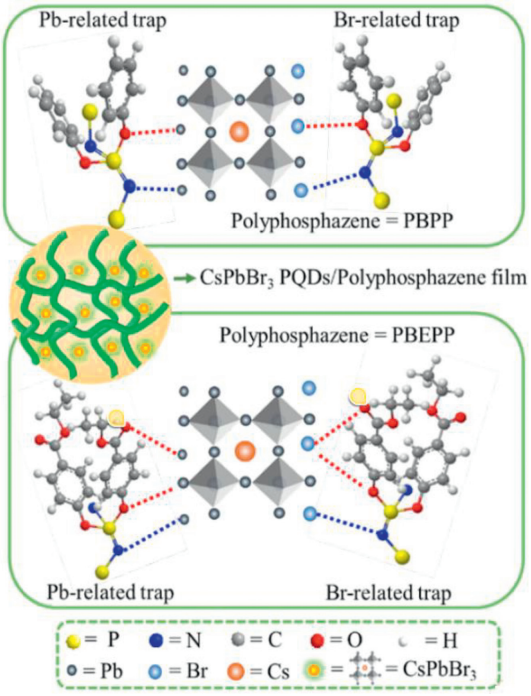

Fig. 6. Schematic illustration of the interactions between PBPP and $CsPbBr_3$ PQDs, PBEPP and $CsPbBr_3$ PQDs.

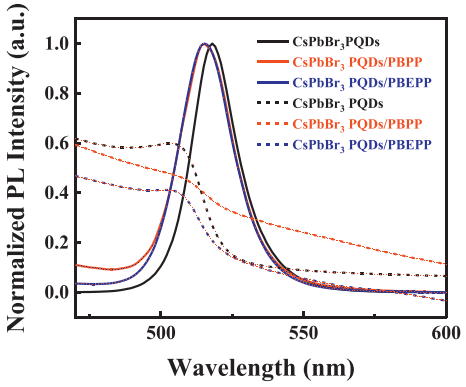

Fig. 7. PL and UV absorption spectra of $CsPbBr_3$ PQDs, CsPbBr3 PQDs/PBPP and CsPbBr3 PQDs/PBEPP thin film.

Fig. 7 shows the UV absorption and photoluminescence (PL) spectra of $CsPbBr_3$ PQDs, $CsPbBr_3$ PQDs/PBPP, and $CsPbBr_3$ PQDs/PBEPP. The intrinsic emission peak of $CsPbBr_3$ PQDs appears at 518 nm as green fluorescence. However, upon the location of PBPP and PBEPP matrix, the emission peak has shifted to 515 nm. The UV absorption peaks of $CsPbBr_3$ PQDs, $CsPbBr_3$ PQDs/PBPP, and $CsPbBr_3$ PQDs/PBEPP are observed at 508, 506 and 506 nm, respectively. Therefore, the introduction of polyphosphazenes results in a slight blue shift in both emission and absorption wavelengths of $CsPbBr_3$ PQDs. The decrease in emission wavelength indicates a smaller size of $CsPbBr_3$ PQDs, which further explains that the steric effect related to substituents of polyphosphazenes and the interaction between Br/Pb and N/O together to inhibit the aggregation of the PQDs.

To further investigate the impact of the interaction between $CsPbBr_3$ and polyphosphazenes with different side-group structures on the excited state properties, the photoluminescence (PL) decay lifetime of different samples was measured using a time-resolved PL apparatus, and the charge recombination dynamics of

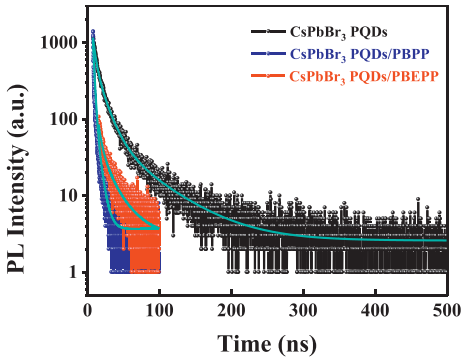

Fig. 8. PL lifetime curves of $CsPbBr_3$, $CsPbBr_3$ PQDs/PBPP and $CsPbBr_3$ PQDs/PBEPP.

Table 1
PL lifetime and fitted values of $CsPbBr_3$ PQDs, $CsPbBr_3$ PQDs/PBPP and $CsPbBr_3$ PQDs/PBEPP.

Sample	$CsPbBr_3$	$CsPbBr_3$/PBPP	$CsPbBr_3$/PBEPP
A1	0.28	0.35	0.21
A2	0.50	0.46	0.43
A3	0.22	0.19	0.37
τ_1	2.81	0.47	0.63
τ_2	12.24	2.66	3.46
τ_3	55.93	12.58	16.95
τ_{avg}	39.85	8.87	14.14

$CsPbBr_3$, $CsPbBr_3$ PQDs/PBPP and $CsPbBr_3$ PQDs/PBEPP were studied (Fig. 8). Three exponential decay functions were used to fit all the curves, and the average PL lifetime of the samples was calculated using Eqs. 1 and 2. The detailed values of τ_1, τ_2 and τ_3 are summarized in Table 1. The fastest lifetime (τ_1) corresponds to the inherent radiative constant from the singlet excited state. In contrast, the other lifetimes (τ_2 and τ_3) are related to long-lived luminescence due to the multiple trapping and detrapping of carriers at the shallow trap states.

$$I(t) = I_0 + A_1\exp\left(-\frac{t}{\tau_1}\right) + A_2\exp\left(-\frac{t}{\tau_2}\right) + A_3\exp\left(-\frac{t}{\tau_3}\right) \quad (1)$$

$$\tau_{avg} = \frac{A_1\tau_1^2 + A_2\tau_2^2 + A_3\tau_3^2}{A_1\tau_1 + A_2\tau_2 + A_3\tau_3} \quad (2)$$

We observed that the average PL lifetimes (τ_{avg}) of $CsPbBr_3$ PQDs/PBPP and $CsPbBr_3$ PQDs/PBEPP have decreased in comparison with the pristine $CsPbBr_3$ PQDs: The τ_{avg} values of 8.87 ns and 14.14 ns are obtained in $CsPbBr_3$ PQDs/PBPP and $CsPbBr_3$ PQDs/PBEPP, both of which are shorter than the τ_{avg} of 39.85 ns in the pristine $CsPbBr_3$ PQDs. This result indicates that $CsPbBr_3$ PQDs/PBPP and $CsPbBr_3$ PQDs/PBEPP composite films have a lower density of surface trap states and faster charge extraction rates compared to pristine $CsPbBr_3$ PQDs [36]. This suggests that polyphosphazenes can effectively passivate surface defects of the perovskite and reduce energy loss. The charge transfer rate of $CsPbBr_3$ PQDs/PBPP is higher than $CsPbBr_3$ PQDs/PBEPP, which is because PBEPP can provide two coordination sites (phenoxy and ester). Therefore, the fluorescence lifetime of PBPP is shorter. These are consistent with the fact that the short-chain aromatic or conjugated ligands capped on PQDs can facilitate exciton delocalization. Fig. 8 illustrates the interfacial structures of $CsPbBr_3$ PQDs/PBPP and $CsPbBr_3$ PQDs/PBEPP, where PBPP or PBEPP can suppress radiative recombination due to facilitation of migration and separation of photogenerated carriers.

The polyphosphazene matrix forms a dense protection layer on the surface of PQDs, effectively inhibiting the interaction with surrounding environment and preventing structural damage. To evaluate the water resistance of the polyphosphazene-$CsPbBr_3$ PQDs

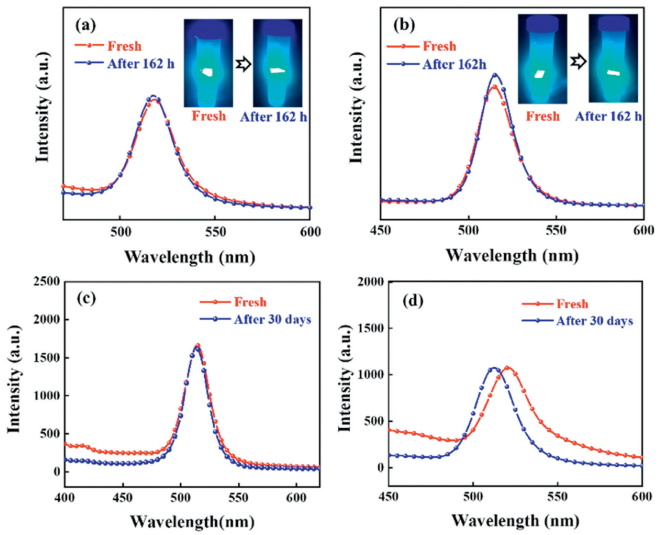

Fig. 9. Long-term PL stability tests of (a) $CsPbBr_3$ PQDs/PBPP and (b) $CsPbBr_3$ PQDs/PBEPP films after soaking in water for 0–162 h. (c) $CsPbBr_3$ PQDs/PBPP and (d) $CsPbBr_3$ PQDs/PBEPP films PL spectra after keeping in the air for 0–30 days and their corresponding photographs under UV (365 nm) light.

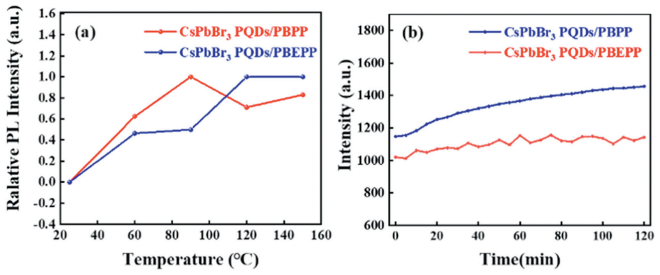

Fig. 10. Long-term stability tests of the $CsPbBr_3$ PQDs/PBPP and $CsPbBr_3$ PQDs/PBEPP thin film. (a) PL intensity under UV (365 nm) light at 25, 60, 90, 120 and 150 °C for 10 min. (b) PL intensity after keeping under 365 nm UV light for 2 h.

composite, the two samples have been dispersed in pure water directly for water stability testing. Periodic collection of the PL emissions of the two samples was conducted, and the spectra are shown in Figs. 9a and b. After immersing samples in water for 162 h, the fluorescence intensity of both samples has increased. In particular, $CsPbBr_3$ PQDs/PBEPP exhibited a more pronounced increase of 10%. This can be attributed to the hydrophilic ester groups of PBEPP, which act as sacrificial layers, preventing water penetration into the active layer. Moreover, trace amounts of water can passivate the surface traps of $CsPbBr_3$ PQDs and enhance the fluorescence intensity. As displayed in Figs. 9c and d, it can be observed that the fluorescence intensity of both composite films has no decrease after 30 days in air. However, there is a blue shift in the emission peak of $CsPbBr_3$ PQDs/PBEPP, which could be attributed to the weaker hydrophobicity of PBEPP compared to PBPP. Oxygen and water in the air can result in the structural changes in $CsPbBr_3$ PQDs, and thus leading to a blue shift of the emission peak.

$CsPbBr_3$ PQDs is regarded as an important material of light-emitting device, the structures are easily destroyed under high temperature conditions, which was an impediment to its application. Additionally, at higher temperatures, thermal stress amplifies the effects of oxygen, light, humidity and other environmental factors on $CsPbBr_3$ PQDs. The different composite films were kept at 25, 60, 90, 120 and 150 °C for 10 min and cooled down to room temperature. Then thermal stability of the film was tested. As shown in PL testing results (Fig. 10a), it can be seen that as the temperature increases, the fluorescence intensity of $CsPbBr_3$ PQDs/PBPP and $CsPbBr_3$ PQDs/PBEPP exceeded the original fluorescence intensity. The fluorescence intensity of $CsPbBr_3$ PQDs/PBPP increased by up to 98% at 120 °C, and the fluorescence intensity of $CsPbBr_3$ PQDs/PBEPP increased by up to 98% at 150 °C. This indicates that polyphosphazenes, as a polymer matrix, can improve the thermal stability of $CsPbBr_3$ PQDs. The fluorescence enhancements of PBEPP are more outstanding at higher temperature. Such enhancement is related to the high charge transfer ability of the aryloxy group in polyphosphazenes, which effectively receives excitation energy from $CsPbBr_3$ and transfers it to polyphosphazenes. The interaction between the C=O group in PBEPP with $CsPbBr_3$ enhances the energy transfer mechanism above 120 °C, resulting in stronger fluorescence intensity. The poor photostability of PQDs also limits their practical applications in the optoelectronics field. Long-term exposure to UV light, PQDs can cause halide ion migration, which further leading to ligand dissociation and crystal regeneration. Fig. 10b shows the fluorescence intensity of both $CsPbBr_3$ PQDs/PBPP and $CsPbBr_3$ PQDs/PBEPP gradually increases by 46.5% and 7%, respectively, upon 365 nm UV light irradiation for 2 h [37,38]. This can be attributed to the UV resistance characteristics of polyphosphazenes, which effectively protects $CsPbBr_3$. The photoinduction effect enhances the passivation of trap states in polyphosphazene, which could suppress non-radiative recombination and quenching phenomena [37,38]. Due to the coordination structure between PBPP-$CsPbBr_3$ and PBEPP-$CsPbBr_3$, $CsPbBr_3$ PQDs/PBPP exhibits a stronger photoinduction effect on $CsPbBr_3$ compared to $CsPbBr_3$ PQDs/PBEPP.

In conclusion, by employing linear polyphosphazenes with phenoxy or 4-ester-phenoxy as pendent groups, we have successfully encapsulated $CsPbBr_3$ PQDs in flexible polymer films, namely $CsPbBr_3$ PQDs/PBPP and $CsPbBr_3$ PQDs/PBEPP. These composite films exhibit excellent dispersion of PQDs, optical transparency and stability in various extreme conditions. The different coordinating groups provided by polyphosphazenes side group lead to various effects on the optical performance and stability of $CsPbBr_3$ PQDs. $CsPbBr_3$ PQDs/PBPP demonstrates excellent air and light stabilities, while $CsPbBr_3$ PQDs/PBEPP shows superior water and thermal resistances. Both composite films all maintain stable fluorescence after a 30-day air storage, but the emission wavelength of $CsPbBr_3$ PQDs/PBEPP shifts towards the blue. Under UV (365 nm) light, the fluorescence intensity of both films is improved. $CsPbBr_3$ PQDs/PBEPP display a greater increase than $CsPbBr_3$ PQDs/PBPP in fluorescence intensity. And $CsPbBr_3$ PQDs/PBEPP also shows a 10% increase in fluorescence intensity after 96 h of water immersion, while $CsPbBr_3$ PQDs/PBPP remains stable. Moreover, under high temperature conditions, the fluorescence intensity of obtained composite film is stronger than room temperature, $CsPbBr_3$ PQDs/PBEPP showing a 98% increase at 150 °C. Therefore, these composite films demonstrate promising capabilities in preventing humidity, UV radiation, oxygen and heat, and holding a strong potential for photo functional and optical applications.

Declaration of competing interest

The authors declare that they have no known competing financial interests or personal relationships that could have appeared to influence the work reported in this paper.

Acknowledgments

This work is supported by the National Science Foundation (NSF) of China (No. 51773010), the Weifang Science and Technology Development Plan Program (No. 2023GX005).

Supplementary materials

Supplementary material associated with this article can be found, in the online version, at doi:10.1016/j.cclet.2024.109795.

References

[1] P. Kambhampati, J. Phys. Chem. Lett. 12 (2021) 4769–4779.
[2] M.A. Cotta, ACS Appl. Nano Mater. 3 (2020) 4920–4924.
[3] N. Hao, Y. Qiu, J. Lu, Chin. Chem. Lett. 32 (2021) 2861–2864.
[4] C. Zhang, T. Li, L. Pu, Chin. Chem. Lett. 31 (2020) 2499–2502.
[5] W. Liu, H. Xie, X. Guo, Opt Mater. 136 (2023) 113398.
[6] Z. Wang, R. Fu, F. Li, Adv. Funct. Mater. 31 (2021) 2010009.
[7] N. Kumar, J.N. Rani, R. Kurchania, Sol Energy 221 (2021) 197–205.
[8] D. Yan, T. Shi, Z. Zang, Small 15 (2019) 1901173.
[9] J.H. Cha, J.H. Han, W. Yin, J. Phys. Chem. Lett. 8 (2017) 565–570.
[10] A.S. de León, M. de la Mata, I.R. Sanchez-Alarcon, ACS Appl. Mater. Interfaces 14 (2022) 20023–20031.
[11] Z.J. Li, E. Hofman, J. Li, et al., Adv. Funct. Mater. 28 (2018) 1704288.
[12] C. Wang, Y. Long, X. Liu, J. Mater. Chem. C 8 (2020) 17211–17221.
[13] H. Lin, Q. Wei, K.W. Ng, Small 17 (2021) 2101359.
[14] Y. Hu, S. Kareem, H. Dong, ACS Appl. Nano Mater. 4 (2021) 6306–6315.
[15] H. Kim, S. So, A. Ribbe, Chem. Commun. 55 (2019) 1833–1836.
[16] H. Kim, N. Hight-Huf, J.H. Kang, Angew. Chem. Int. Ed. 59 (2020) 10802–10806.
[17] J. He, A. Towers, Y. Wang, Nanoscale 10 (2018) 15436–15441.
[18] J. Qiu, W. Xue, W. Wang, Dyes Pigments 198 (2022) 109–806.
[19] Z. Miao, D. Yan, X. Wang, Chin. Chem. Lett. 33 (2022) 4026–4032.
[20] F. Yang, M. Qiu, Z. Miao, ACS Appl. Mater. Interfaces 13 (2021) 29894–29905.
[21] Z. Miao, D. Yan, T. Zhang, ACS Appl. Mater. Interfaces 13 (2021) 32094–32105.
[22] Z. Ali, M. Basharat, Z. Wu, ChemElectroChem 8 (2021) 759–782.
[23] M. Basharat, Y. Abbas, D. Hadji, J. Mater. Chem. C 8 (2020) 13612–13620.
[24] M. Basharat, Y. Abbas, W. Liu, Polymer 185 (2019) 121942.
[25] M. Basharat, D. Hadji, J. Mater. Sci. 57 (2022) 6971–6987.
[26] M. Basharat, Z.H. Shah, M. Ikram, Small 18 (2022) 2107621.
[27] R.J. Davidson, E.W. Ainscough, A.M. Brodie, Eur. J. Inorg Chem. 2010 (2010) 1619–1625.
[28] C.J. Orme, J.R. Klaehn, F.F. Stewart, J. Membrane Sci. 238 (2004) 47–55.
[29] R.S. Ullah, L. Wang, H. Yu, RSC Adv. 7 (2017) 23363–23391.
[30] Y.J. Cheng, S.H. Yang, C.S. Hsu, Chem. Rev. 109 (2009) 5868–5923.
[31] J. Zhou, H. Lin, Y. Yu, Chem. Eur. J. 26 (2020) 10528–10533.
[32] R. Wycisk, P.N. Pintauro, W. Wang, J. Appl. Polym. Sci. 59 (10) (2015) 1607–1617.
[33] F. Yang, Shuangkun Yang, Yang Liu, Electrochim. Acta 328 (2019) 135064.
[34] J. Zhang, P. Jiang, Y. Wang, ACS Appl. Mater. Interfaces 12 (2020) 3080–3085.
[35] Y. Sun, J. Zhang, H. Yu, ACS Appl. Mater. Interfaces 14 (2022) 6625–6637.
[36] H.P. Zeng, Y. Zhao, X. Wang, Chem. Engin. J. 435 (2022) 134867.
[37] C. Carrillo-Carrion, S. Cardenas, B.M. Simonet, Chem. Commun. (2009) 5214–5226.
[38] S. Chu, S. Pan, G. Li, Phys. Chem. Chem. Phys. 20 (2018) 25476–25481.